Int. J. Heat Mass Transfer. Vol. 25, No. 11, pp. 1709–1718, 1982
Printed in Great Britain

0017–9310/82/111709–10 $03.00/0
Pergamon Press Ltd.

NUMERICAL COMPUTATIONS OF WALL-JET FLOWS

R. N. SHARMA
Chemical Engineering Department, Indian Institute of Technology, Kanpur-208016, India

and

S. V. PATANKAR
Mechanical Engineering Department, University of Minnesota, Minneapolis, MN 55455, U.S.A.

(*Received* 9 *November* 1978 *and in final form* 25 *March* 1982)

Abstract—Turbulent wall-jets on conical surfaces represent a practically useful situation and an important test for theoretical methods used for predicting turbulent transport. Experimental data on the velocity fields and the maximum concentration of a tracer gas have been obtained for turbulent wall-jets formed on conical surfaces of various angles. It is shown that the correct prediction of the data by a mixing-length hypothesis requires the mixing-length constant to be changed for each cone angle. A set of two-equation models of turbulence is then employed which solves two additional differential equations for the local properties of turbulence. These models correctly predict all the experimental data without the need for the adjustment of constants.

NOMENCLATURE

a, initial radius of the conical geometry (at the slot);
c, constant in the expression for jet-spread rate;
C_1, C_2, C_D, constants;
C_w, tracer gas concentration at the surface;
J_j, effective diffusive flux of species j;
k, kinetic energy of fluctuations per unit mass;
K, empirical constant in PML model;
l, length-scale in PML model of turbulence;
L, length-scale in two-equation turbulence models;
m_j, mass fraction of the species j in the fluid stream;
m_E, mass transfer rate across a boundary;
PML, Prandtl Mixing Length;
r, distance from the axis of symmetry;
r_E, distance from the axis of symmetry to the edge of the boundary layer;
u, v, mean velocity in x and y directions, respectively;
U_c, velocity at the slot;
U_{max}, maximum velocity;
x, y, streamwise and cross-stream distances along and from solid boundary;
y_c, slot-width;
y_l, characteristic thickness of the boundary layer;
$y_{1/2}$, value of y corresponding to half of the maximum velocity;
Z, turbulence property, a combination of k and L.

Greek symbols

α, angle between the main flow direction and the axis of symmetry (also represents the half-angle of the conical geometry);
σ_j, effective Schmidt number;
σ_k, σ_Z, constants;
δ, boundary layer thickness;
μ_{eff}, effective viscosity, empirical constant in PML models;
λ, empirical constant in PML model;
ρ, density of the jet-fluid (air);
τ, effective shear stress.

1. INTRODUCTION

THE FLOW configuration of a fluid jet impinging on a target surface occurs in a variety of engineering situations and forms the basis of the wall-jet, which may be described as a jet blown through an injection slot over a solid surface. When the jet impinges normal to a flat surface and spreads out radially along the surface, the resulting flow development is termed a radial wall-jet. A plane wall-jet would occur if the jet was blown tangentially to a flat surface. Published literature deals primarily with these two types of wall-jet. Starr and Sparrow [1], and Manian *et al.* [2] have reported investigations on a cylindrical wall-jet. A cylindrical wall-jet is created when a jet emerges from an annular slot and flows longitudinally and co-axially over a cylindrical surface.

In the present study, a continuous geometrical transition was conceived as including conical wall-jets between plane and radial wall-jets, where α, the angle between the main flow direction and the axis of symmetry, changed continuously from 0 to 90°. The cylindrical wall-jet ($\alpha = 0$) would approximate to a plane wall-jet if the radius of the cylinder becomes very large. A conical wall-jet can, therefore, be defined as a jet blown through an annular slot along a conical surface.

1.1. *Motivation and objective of the present study*

The practical need for computation of turbulent flows is pressing notwithstanding the fact that the known mechanism of turbulent transfer is still not fully comprehensive. Various turbulence models have been proposed. The primary function of a turbulence model is to calculate effective viscosity, μ_{eff}, if the turbulent-exchange laws are taken equivalent in form to the Newton's Law of Viscosity for a laminar flow, i.e. the effective shear stress, τ, representing the sum of laminar and turbulent shear stresses may be expressed as

$$\tau = \mu_{\text{eff}} (\partial u/\partial y) \tag{1.1}$$

where $\partial u/\partial y$ is the velocity gradient. It is in this context, that, of late, shortcomings of Prandtl Mixing Length (PML) model, which expresses μ_{eff} as a function of a length scale (l) and a local velocity gradient, have been recognized. This length scale l is expressed in terms of the constants K and λ. With the help of a simple mass and momentum balance, it can be shown that the values of these constants for the radial wall-jet case are $2^{1/2}$ times their values for the plane wall-jet case i.e.

$$(K, \lambda)_{\text{radial}} = 2^{1/2} (K, \lambda)_{\text{plane}}. \tag{1.2}$$

The motivation for selecting the present flow-system came from the hypothesis that the abrupt changes in (K, λ)-values, as represented by equation (1.2), should be, in fact, continuous, to give rise, as mentioned earlier, to a set of conical wall-jets.

The conical wall-jets, though apparently similar, offer continuously varying flow situations with the key variable, α, assuming different values. This provides a convenient, yet critical, testing ground for the universal validity of a turbulence model. Universality implies that a single set of empirical constants, inserted in the equations, would provide satisfactory predictions for a large variety of flows. Basically the purpose of the present study is to assess and establish the universal character of a class of turbulence models (two-equation turbulence models) against the varying flow situations of conical wall-jets. It is neither the purpose of the present study to develop a turbulence model nor to modify or sophisticate the existing ones.

The models, therefore, have been used in forms as reported. A brief mention of the models used would be appropriate and is, therefore, included. An excellent survey of existing turbulence models have been given by Rodi and Spalding [3]. Recently, Launder and Spalding [4] have given the main concepts and have discussed these models together with their application to divergent flow situations.

2. THE TURBULENCE MODELS

The PML model and two-equation turbulence models have been used for predictions and subsequent comparisons with experimental data. The simple and the most widely used PML model is examined first.

2.1. *Prandtl mixing length (PML) model and its use for conical wall-jets*

According to the PML model, the effective viscosity is given by the expression

$$\mu_{\text{eff}} = \rho l^2 |\partial u/\partial y|. \tag{2.1}$$

In the present context of wall-jets which are essentially either 2-dim. or axisymmetric boundary layers along a single wall, the distribution of l is taken after the recommendations of Escudier [5]

$$l = Ky; \qquad y \le (\lambda/K)\, y_1 \tag{2.2}$$

and

$$l = \lambda y_1; \qquad y > (\lambda/K)\, y_1 \tag{2.3}$$

where y_1 is a characteristic thickness of the boundary layer.

A typical flow configuration of a conical wall-jet is shown in Fig. 1. It can be assumed without incurring serious error that the momentum lost in the thin wall region can be neglected in comparison to the total momentum at any stream station x. Thus

$$\frac{\mathrm{d}}{\mathrm{d}x} \int_0^\delta \rho u^2 2\pi r \mathrm{d}y = 0 \tag{2.4}$$

where r, the distance from the axis of symmetry to a point in the boundary layer, called local radius, is given by

$$r = a + x\sin\alpha + y\cos\alpha \tag{2.5}$$

and u, following similarity of velocity profiles, can be represented as

$$\frac{u}{u_{\max}} = f(y/\delta). \tag{2.6}$$

Sharma [6] has observed similarities in the velocity profiles up to a distance of 0.06 cm from the wall. It is assumed that the profile extends right up to the wall and, therefore, momentum lost at the wall is not accounted for, as mentioned earlier, and has been neglected. Equation (2.4) can now be integrated to give

$$u_{\max}\left[(a + x\sin\alpha)\,\delta\frac{I_{\text{m}}}{I'_{\text{m}}} + \delta^2\cos\alpha\right]^{1/2} = \text{const.} \tag{2.7}$$

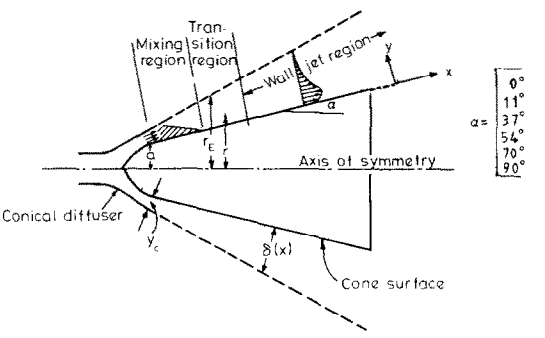

FIG. 1. A typical conical wall-jet flow system.

where

$$I_m = \int_0^1 f^2 \, d\eta,$$

$$I'_m = \int_0^1 f^2 \, \eta d\eta,$$

$$\eta = (y/\delta).$$

Next, a mass balance is taken at any x

$$\frac{d}{dx} \int_0^\delta \rho u \, 2\pi r dy = -2\pi r_E m_E \qquad (2.8)$$

where m_E is the mass of fluid entrapped from the surroundings per unit length of the boundary layer periphery, and r_E is the distance from the axis of symmetry to the edge of boundary layer. With proper substitutions for u and r, equation (2.8) reduces to

$$\frac{d}{dx}\left(U_{max}\left[(a + x \sin\alpha)\delta \frac{I_Q}{I'_Q} + \delta^2 \cos\alpha\right]\right) = -\frac{r_E m_E}{\rho I'_Q} \qquad (2.9)$$

where

$$I_Q = \int_0^1 f \, d\eta$$

and

$$I'_Q = \int_0^1 f\eta d\eta.$$

For the given flow situation, the following approximation is used

$$\frac{I_Q}{I'_Q} = \frac{I_m}{I'_m} \qquad (2.10)$$

and also, for a constant jet-spread rate which is independent of α

$$\delta/x = c \qquad (2.11)$$

where c is a constant.

With the help of equations (2.7), (2.10) and (2.11), equation (2.9) finally reduces to

$$\frac{1/2[ac + 2(I_m/I'_m)cx \sin\alpha + 2c^2 x \cos\alpha]}{(a + x \sin\alpha + cx \cos\alpha)} = \frac{-m_E}{\rho U_{max} I'_Q}. \qquad (2.12)$$

From the expression of entrainment at the free boundary, the term $m_E/(\rho U_{max})$ can be taken as proportional to λ_α^2, where λ_α is the constant corresponding to a specified value of α. Thus, the ratio of the constants for the radial wall-jet ($\alpha = 90°$), where x is sufficiently large so that a can be neglected in equation (2.12) and plane wall-jet ($\alpha = 0$, $a = \infty$) would be

$$\frac{\lambda_{radial}}{\lambda_{plane}} = \frac{K_{radial}}{K_{plane}} = 2^{1/2}. \qquad (2.13)$$

For any other values of α, at large values of x

$$\frac{\lambda_\alpha}{\lambda_{90}} = \left[\frac{1 + c(I'_m/I_m)\cot\alpha}{1 + c\cot\alpha}\right]^{1/2} = \frac{K_\alpha}{K_{90}}. \qquad (2.14)$$

It can be inferred from the foregoing approximate analysis that K and λ are not, in fact, universal constants since they depend on the apex angle of the cone. The PML model is, therefore, not quite adequate to be employed in predictions for conical wall-jet flows with a constant set of values for K and λ. Predictions based on the PML model and comparisons with the data are discussed later.

2.2. *Two-equation models of turbulence*

Kolmogorov [7], Prandtl [8] and Emmons [9] independently proposed that the local state of turbulence of a fluid can be characterised by only two quantities, the kinetic energy of the turbulent velocity fluctuations k, and a length scale L. On the basis of this concept, μ_{eff} can be expressed in the following form:

$$\mu_{eff} = \rho k^{1/2} L. \qquad (2.15)$$

The main characteristic of the two-equation model is that k and L are determined by differential equations describing the transport of k and L separately. If k is already calculated, then the dependent variable for the second equation could instead be a variable Z, made up of a combination of k and L, defined in the following way:

$$Z = k^m L^n \qquad (2.16)$$

where m and n are exponents. Three principal models of this type have been investigated in the present study. It is essentially the form of Z, which distinguishes one model from the other. Table 1 specifies the forms in which Z is chosen.

3. MATHEMATICAL FORMULATION

The wall-jet flows under consideration are essen-

Table 1. Expressions for Z

Model	Reference	Form of Z	Physical interpretation
k–kL	[10] Ng and Spalding	kL	Energy length scale product
k–w	[11] Spalding	k/L^2	Square of characteristic frequency of energy containing eddies
k–ε	[12] Jones and Launder	$k^{3/2}/L$	Kinematic dissipation rate of turbulence energy

Table 2. Expressions for S

Z	S
kL	$-[702\ (L/y)^6\ k^{2/3}]$
k/L^2	$3.5\,\mu_{\text{eff}}\,(\partial^2 u/\partial y^2)^2$
$k^{3/2}/L$	0

tially boundary layers. The analysis, therefore, would be for 2-dim. boundary layers neglecting the effects of pressure gradients and body forces. The appropriate coordinate system is sketched in Fig. 1, where the x-coordinate is along the solid boundary, and the y-coordinate normal to it. The governing differential equations are as follows:

Conservation of mass

$$\frac{\partial}{\partial x}(\rho u r) + \frac{\partial}{\partial y}(\rho v r) = 0. \tag{3.1}$$

Conservation of momentum in x*-direction*

$$\rho u \frac{\partial u}{\partial x} + \rho v \frac{\partial u}{\partial y} = \frac{1}{r}(\tau r). \tag{3.2}$$

Conservation of chemical species j

$$\rho u \frac{\partial m_j}{\partial x} + \rho v \frac{\partial m_j}{\partial y} = \frac{1}{r}\frac{\partial}{\partial y}(J_j r) \tag{3.3}$$

where m_j is the mass-fraction of the species j. Its effective diffusive flux, J_j, is expressed in a similar way as τ, i.e.

$$J_j = (\mu_{\text{eff}}/\sigma_j)\frac{\partial m_j}{\partial y} \tag{3.4}$$

where σ_j is the effective Schmidt number, treated as an empirical constant in the present study.

Conservation of turbulent kinetic energy

The 2-dim. boundary layer equation for turbulent kinetic energy, k, can be obtained from the Navier–Stokes equation. The equation so obtained, through a set of approximations due to Prandtl, Kolmogorov etc., is finally reduced to the following term:

$$\rho u \frac{\partial k}{\partial x} + \rho v \frac{\partial k}{\partial y} = \frac{1}{r}\frac{\partial}{\partial y}\left[\frac{r\,\mu_{\text{eff}}}{\sigma_k}\frac{\partial k}{\partial y}\right] + k\left[\frac{\mu_{\text{eff}}}{k}\left(\frac{\partial u}{\partial y}\right)^2 - \frac{C_{\text{D}}\rho^2 k}{\mu_{\text{eff}}}\right]. \tag{3.5}$$

Conservation of Z

Rotta [13] derived the transport equations appropriate to boundary layer flows for the length scale L and kL from general Navier–Stokes equations together with the concept of the statistical behaviour of turbulence. Later on, a general equation for Z was formulated. As pointed out earlier, it is the physical interpretation of Z which differentiates one model from the other. In mathematical representation they are otherwise similar. One form of differential equation can be manipulated to give the other form. Launder and Spalding [4] have discussed the basic concepts of the Z-equation, of which a common form for 2-dim. boundary layer flows, can be written as

$$\rho u \frac{\partial Z}{\partial x} + \rho v \frac{\partial Z}{\partial y} = \frac{1}{r}\frac{\partial}{\partial y}\left[\frac{r\mu_{\text{eff}}}{\sigma_Z}\frac{\partial Z}{\partial y}\right] + Z\left[\frac{C_1\mu_{\text{eff}}}{k}\left(\frac{\partial u}{\partial y}\right)^2 - \frac{C_2\rho^2 k}{\mu_{\text{eff}}}\right] + S \tag{3.6}$$

where σ_Z, C_1 and C_2 in the present study are assumed constants. The additional term S represents secondary source terms which differ according to the physical meaning of the variable Z; the particular forms of S are included in Table 2.

4. SOLUTION PROCEDURE

In order to predict the hydrodynamical properties of interest, the equations for momentum, k and Z must be solved simultaneously together with the auxiliary relation (1.1) and the boundary conditions. For prediction of tracer-gas concentrations, equations (3.3 and 3.4) are also to be included. The equations are parabolic and the solution can be obtained numerically by a finite-difference scheme. In the present case, the finite-difference method of Spalding and Patankar [14], which integrates the equations in a forward-marching procedure, was used.

The differential equations employed for numerical computations contain the terms C_{D}, σ_k, σ_Z, C_1, C_2 and σ_j, which in the absence of definite information have been assumed constant for high Reynolds numbers. The magnitudes of these constants, derived from diverse experimental evidence, have been taken from their quoted values by Launder and Spalding [15], and are shown in Table 3.

The conditions at the free-boundary were taken as follows:

$$y = \delta;\quad u = k = Z = m_j = 0.$$

The details of inner boundary conditions based on Couette-flow analysis and starting profiles needed to initiate the numerical computation can be found in ref. [6] or [10].

5. EXPERIMENTAL PROGRAMME

A general schematic diagram of the experimental set-up is given in Fig. 2. It essentially consists of a given cone geometry pushed into a brass diffuser, with the same apex angle as the cone, to the extent that a desired annular gap-width is created between the diffuser and the cone. Air from the pipe was blown through this annular gap along the surface of the cone, as a wall-jet. A detailed description of the apparatus, alignment and test procedures, sources of error and data reduction is reported by Sharma [6].

Table 3. Magnitudes of numerical constants involved in the differential equations

Dependent variable	C_1	C_2	C_D	σ_k	σ_Z	σ_j
kL	0.98	0.059	0.09	1.0	1.0	
k/L^2	1.04	0.170	0.09	0.9	0.9	
$k^{3/2}/L$	1.45	0.140	0.07	1.0	1.1	
m_j						0.9

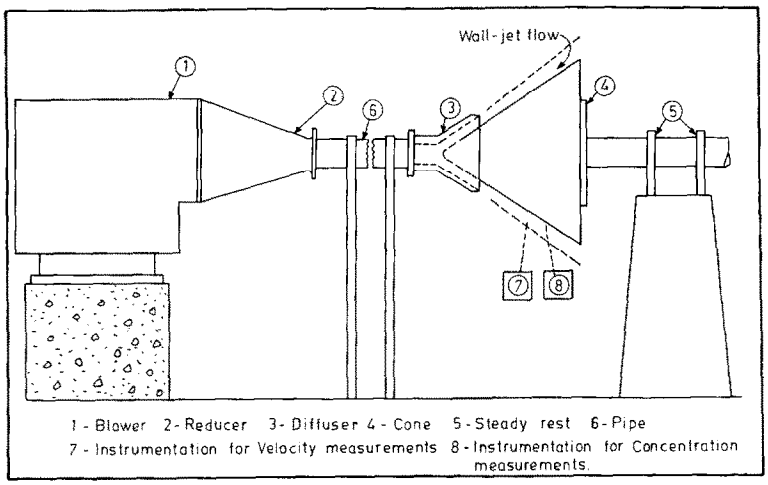

FIG. 2. General arrangement of the experimental set-up.

An experimental investigation was undertaken to generate the following data:

(1) Velocity profile measurements at various distances from the slot along the surface of different conical wall-jet systems. The growth rate of the jet and decay of maximum velocity, needed for comparison with the predicted values on the basis of a turbulence model, can be derived from the velocity profile data.

(2) Surface concentration measurements of a tracer gas at different positions along the longitudinal surface of the same set of conical geometries as in (1) above. Acetylene, the tracer gas, was introduced near the inlet length of pipe carrying main air-flow. Since the surface of the conical geometry was impervious and chemically inert, the maxima of concentration profile at a stream position occurred at the surface itself. Therefore, the stream concentrations of the tracer gas measured at the surface, in fact, represent the maximum concentration of the gas at the given position.

6. RESULTS AND DISCUSSION

In order to compare with the experimental data, the predictions have been reduced to represent the following properties:

(1) Rate of jet-spread.
(2) Axial decay of maximum velocity.
(3) Dimensionless velocity profiles.
(4) Axial decay of maximum concentration of the tracer gas.

All the comparisons of theoretical and experimental results have not been shown because of repetitive trends. Instead, results for all the 5 cone-geometries corresponding to one slot-width of the order of 0.3 cm have been given, although the generality of results has been emphasized at appropriate places. Also, the characteristic findings for the predictions based on the PML model have been grouped separately to bring forth its inherent limitations, at least in reference to the present flow systems.

Figure 3 depicts the jet-spread for the 5 cone-geometries. It can be observed that the predictions based on the k–w model fit the data better. This observation, however, is not generally true with respect to data of the remaining slot-widths. Qualitative agreement of the predictions based on two-equation models with the corresponding data are summarized in Table 4, where the degree of agreement has been labelled with expressions like poor, satisfactory, fair, good or excellent. Reference to these labels could be drawn from Fig. 3. A scrutiny of the table suggests that the two-equation models possess the universal character for jet-spread predictions. With an overview for the given conditions, the k–ε model seems to have more potential.

Figure 4 shows the comparisons for u_{max}-decay. The extent of agreement, in terms similar to those used for jet-spread, are also included in Table 4 to which Fig. 4 serves as a reference. An examination of the table here

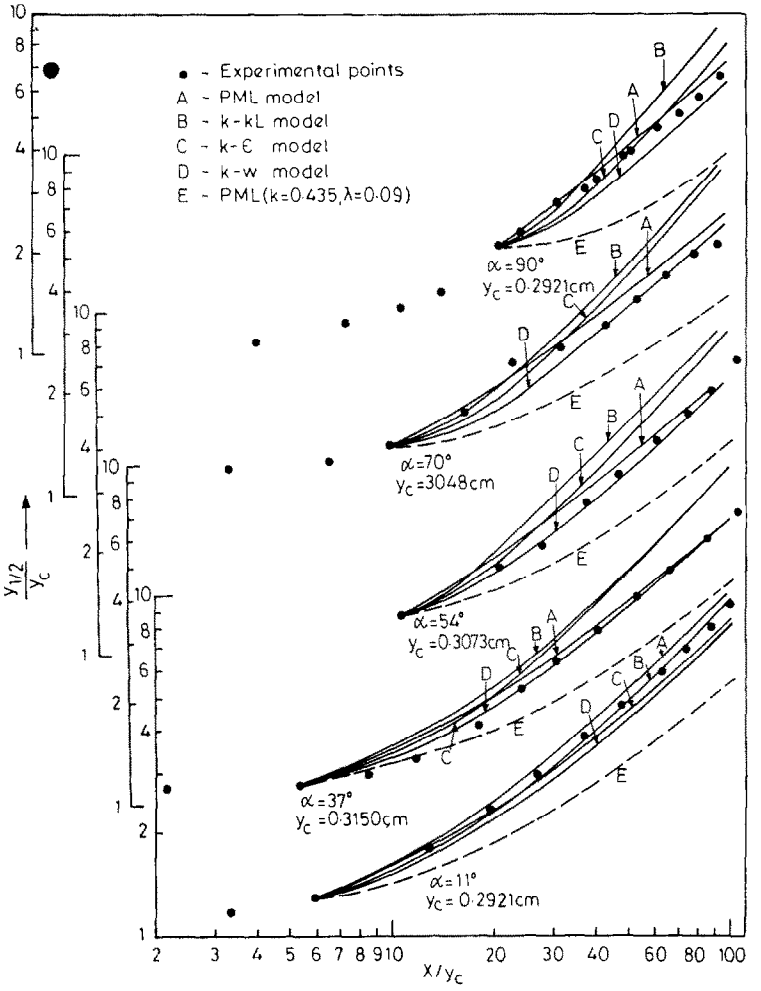

FIG. 3. Jet-spread.

also suggests that the universal character of the two-equation models is retained and, as in the case of jet-spread, the k–ε model on the whole seems to make better predictions.

Velocity profiles, experimental and theoretical, for a typical cone-geometry ($\alpha = 54°$) are shown in Fig. 5. It can be observed that there is not much difference in the predicted velocity profiles and they compare well with the experimental profiles. Similar trends were observed in the comparisons when profiles for the rest of the flow systems were studied. It should be noted that the computational method presumes an empirical velocity profile in the wall region. Therefore, comparisons of the profile in the wall region are without any purpose as they are same and not unique to any turbulence model.

Theoretical profiles of k and L are not included for discussion since, in the absence of relevant data, no comparisons were possible.

The streamwise decay of the maximum concentration of the tracer gas (C_w) is shown in Fig. 6. It is evident that all the turbulence models are successful in predicting the C_w-decay within acceptable limits of accuracy. The results of comparisons between the predicted and experimental decay of maximum concentration are summarized in Table 5. Here too, the predictions follow the earlier patterns.

From the foregoing findings it can be concluded that the two-equation turbulence models are capable of successfully predicting the properties of diverse flows with the same set of constants involved in the differential equations, a situation which lends universal character to the models.

It is evident from Figs. 3, 4 and 6 that fixed values of K and λ (0.435 and 0.09) fail completely to yield satisfactory predictions for the present flow systems. It can be observed that the resulting discrepancies in predictions relatively decrease from 90 to 0° cone angles. When these constants, however, were adjusted for the best fit, keeping the ratio K/λ constant [14], the predicted curves (A) agree well with the experimental data. Additional data taken on a cylinder ($\alpha = 0$), as shown in Fig. 7, further confirm these trends.

The values of these adjusted constants are plotted in Fig. 8 against α. The continuous curve represents the values of K_x or λ_x calculated from equation (2.14). The

Table 4. Qualitative agreement of predicted jet-spread and u_{max}-decay with experimental data, P = poor; S = satisfactory; F = fair; G = good; E = excellent

α (degrees)	y_c (cm)	Agreement of the predicted jet-spread			Agreement of the predicted u_{max}-decay		
		k–kL	k–ε	k–w	k–kL	k–ε	k–w
90.0	0.0991	F	S	P	F	S	P
	0.1956	S	E	P	F	G	P
	0.2921	P	P	S	G	S	P
	0.5842	P	G	P	G	S	P
	1.2573	G	S	P	G	S	P
70.08	0.1016	P	F	P	S	F	P
	0.1956	P	F	P	S	F	P
	0.3048	P	P	G	G	G	P
	0.6350	E	S	P	E	S	P
	1.2700	G	S	P	G	S	P
53.92	0.1029	F	S	S	F	S	S
	0.2057	P	P	P	P	P	S
	0.3073	P	P	F	P	S	S
	0.6058	P	E	P	P	E	P
	1.2725	S	F	P	G	F	P
37.12	0.1016	S	F	P	S	F	P
	0.1956	P	G	P	P	G	P
	0.3150	P	P	G	P	P	G
	0.6210	P	F	P	P	G	P
	1.2650	S	E	P	S	E	S
11.25	0.1016	G	E	P	G	E	P
	0.1965	G	E	P	G	E	P
	0.2921	P	P	S	S	S	P
	0.6020	F	E	P	F	E	P
	1.2624	G	F	P	G	F	P

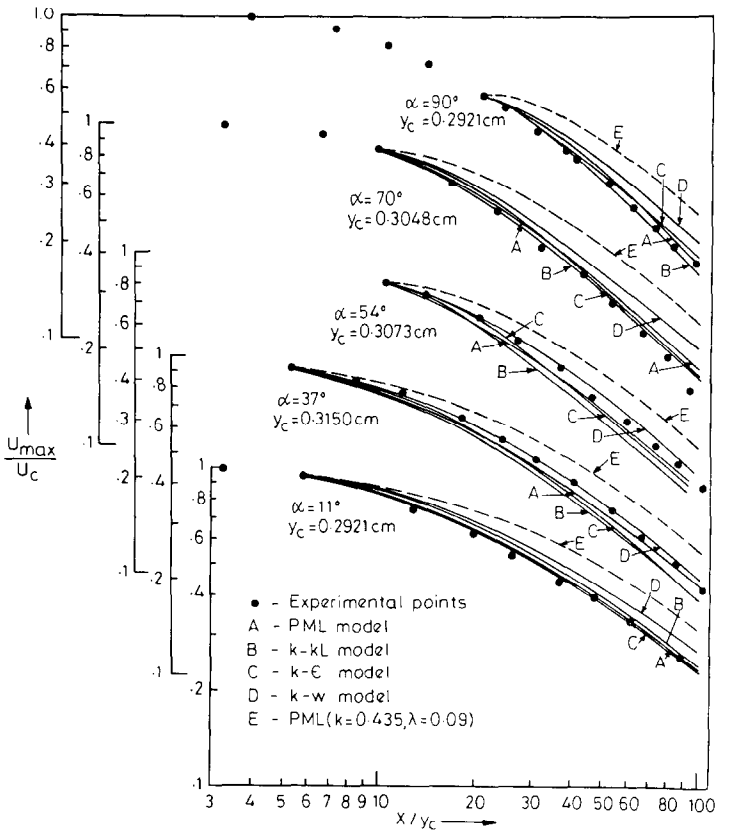

FIG. 4. Decay of maximum velocity.

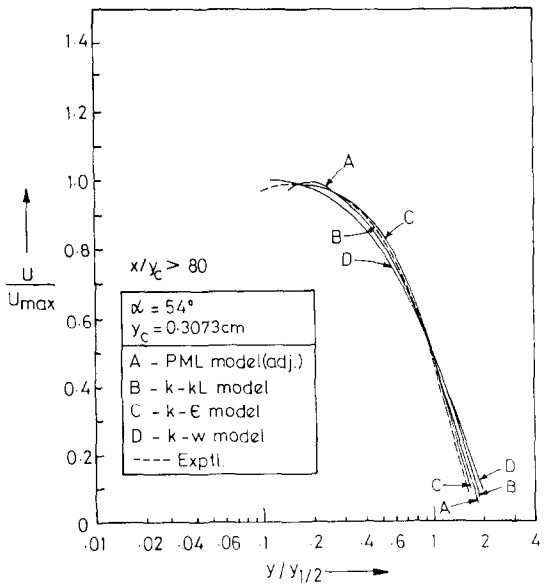

FIG. 5. Velocity profiles.

reference values of the constants for $\alpha = 90°$ were taken as $K = 0.8$ and $\lambda = 0.1$ which are the best adjusted values to fit the present data. Patankar and Spalding [14] also report the same values of these constants for the best fit on their own and Baker's data [16]. It should be recognised that calculated values of K or λ from equation (2.14) would not be satisfactory at smaller values of α as is evident from equation (2.12). The continuous curve is, therefore, extrapolated (dotted line) from about 37°. The extrapolated value of K_x/K_{90} matches fairly well with the experimental value at $\alpha = 0°$. It is anticipated that K/λ would change during the transition from a cylindrical wall-jet to a plane wall-jet ($r \to \infty$) and the major change would be in K rather than in λ since the nature of the free boundary does not change much. This transition, however, requires further study.

Figure 8 illustrates, at least as an approximation, the validity of the analysis culminating in equation (2.14). It is thus clear that K, λ-values vary gradually from one extreme of a conical wall-jet (plane wall-jet) to the other extreme (radial wall-jet). K and λ, therefore, are

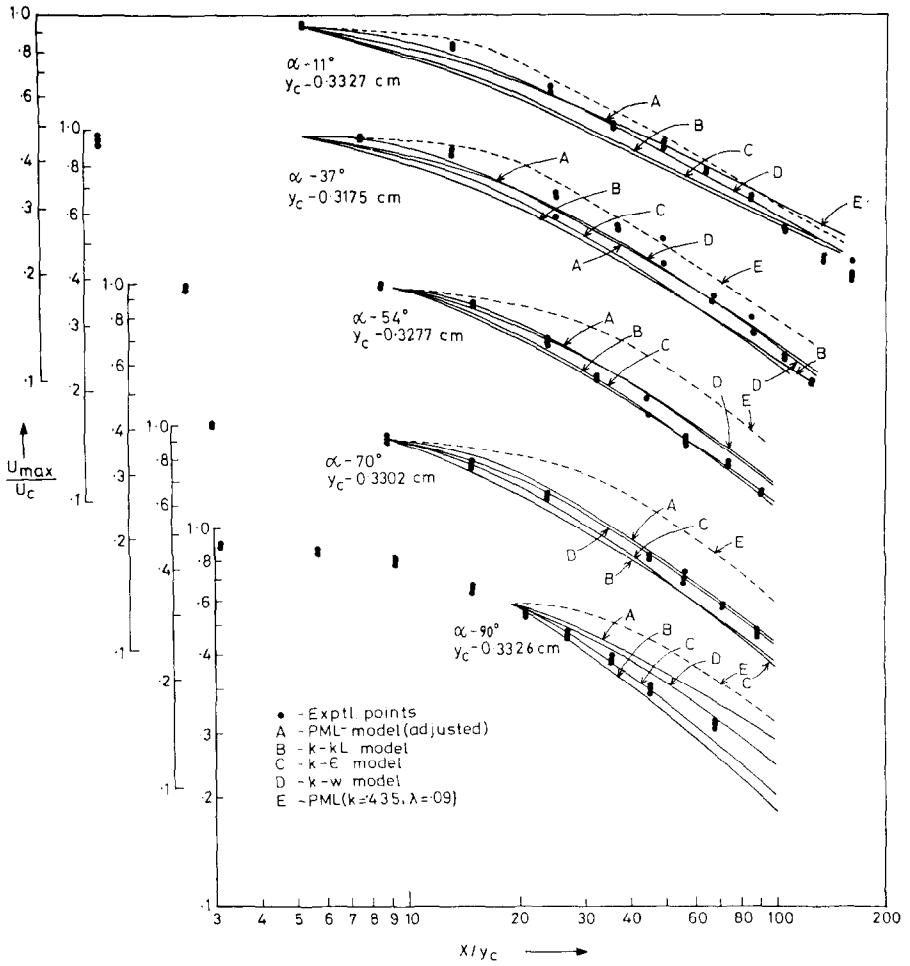

FIG. 6. Decay of maximum concentration of tracer gas.

Table 5. Qualitative agreement of the predicted decay of maximum concentration of the tracer gas (acetylene), P = poor; S = satisfactory; F = fair; G = good; E = excellent

α (degrees)	y_c (cm)	Agreement of the predicted C_w-decay k–kL	k–ε	k–w
90.0	0.3226	S	G	P
	0.6350	G	S	P
	1.2624	F	G	P
70.08	0.3302	P	P	G
	0.6350	G	G	P
	1.2649	S	P	P
53.92	0.3277	G	G	S
	0.6350	F	F	P
	1.2675	S	E	P
37.12	0.3175	P	P	G
	0.6350	S	F	P
	1.2675	S	F	P
11.25	0.3327	S	S	F
	0.6325	S	G	F
	1.2675	P	F	G

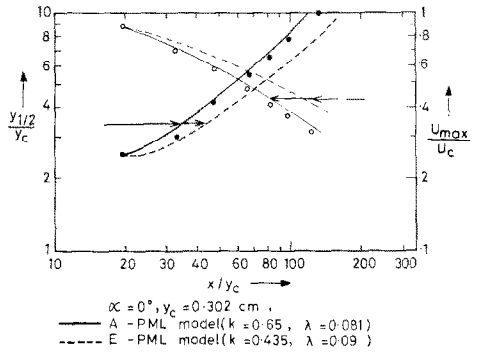

FIG. 7. Jet-spread and decay of maximum velocity.

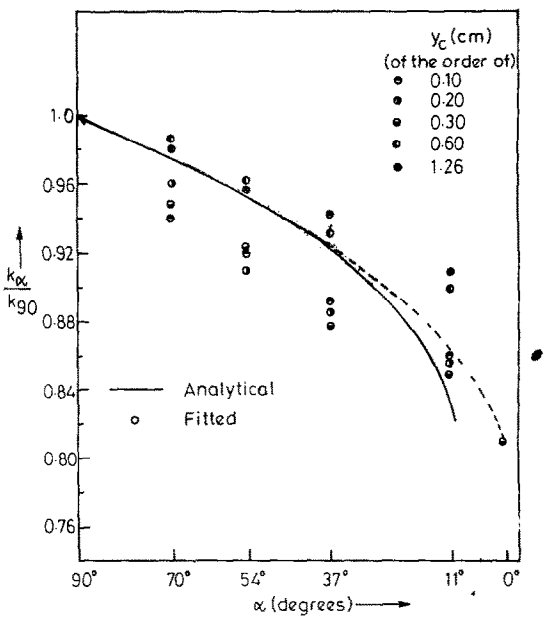

FIG. 8. Comparison of K_α/K_{90}.

not universal constants. Rodi and Spalding [3] have reported similar observations with free-jet studies. This indicates that the underlying model of turbulence lacks some important features. The main cause of this inadequacy probably lies in length-scale specification. Experience has shown that the algebraic specification of l must vary with the nature of the geometry or boundary conditions. This can be accounted for in the PML model only by adjusting the constants. The two-equation turbulence models, on the other hand, turn out to be superior in this regard, because they solve a differential equation for the length-scale and predict, rather than assume, what the length-scale distribution should be.

Finally, it should be noted that the empirical constants C_1, C_2, C_D, σ_k, σ_Z and σ_j are still being tuned by computer optimization of predictions for a wide range of experimentally documented flows. Therefore, till final values are assigned to these constants, an attempt to distinguish the accuracy of predictions of one from the other would be rather premature. The aim of the present study has not been to recommend a particular two-equation model, but instead, as a first step, to establish the universal character of the models; that is to check if the same set of constants involved in different models can successfully predict the properties of diverse flows. And in this respect, the two-equation models do achieve the necessary objective when used to predict the conical wall-jet development.

7. CONCLUSIONS

The two-equation turbulence models, in which the mixing length is not specified algebraically but through a differential equation, can be used as a successful basis for predicting the boundary layer development of different conical wall-jets.

As an auxiliary observation, it can be added that the performance of the k–ε model seems to be encouraging. This, however, is not conclusive since the present study was not directed to evaluate the performance of the different two-equation models.

Also, the PML model is inadequate to predict satisfactorily the properties of conical wall-jets with fixed constants ($k = 0.435$; $\lambda = 0.09$). A correlation has been developed which calculates the value of the constants for different cone geometries. These calculated values agree well with the ones adjusted for the best fit with the experimental data.

REFERENCES

1. J. B. Starr and E. M. Sparrow, Experiments on a turbulent cylindrical wall-jet, *J. Fluid Mech.* **29**, 495–512 (1967).
2. V. S. Manian, T. W. McDonald and R. W. Besant, Heat transfer measurements in cylindrical wall-jets, *Int. J. Heat Mass Transfer* **12**, 673–679 (1969).
3. W. Rodi and D. B. Spalding, A two-parameter model of turbulence and its application to free jets, *Wärme- und Stoffübertragung* **3**, 85–95 (1970).
4. B. E. Launder and D. B. Spalding, *Mathematical Models of Turbulence*. Academic Press, New York (1972).
5. M. P. Escudier, The distribution of the mixing length in turbulent flows near walls, Imperial College, London, Mech. Eng. Dept., Rep. TWF/TN/1 (1965).
6. R. N. Sharma, Momentum and mass transfer in turbulent conical wall-jets, Ph.D. Thesis, Indian Institute of Technology, Chem. Eng. Dept., Kanpur (1972).
7. A. N. Kolmogorov, Equations of turbulent motion of an incompressible fluid, *Izv. Akad. Nauk. SSSR Ser. Phys.* VI, No. 1/2, 56–58 (1942).
8. L. Prandtl, Über ein neues Formelsystem für die ausgebildete Turbulenz, *Nachrichten Akad. Wiss. (Göttingen), Math. Phys.* 6–19 (1945).
9. H. W. Emmons, Shear flow turbulence, *Proc. 2nd US Nat. Congr. Appl. Mech.* ASME (1954).
10. K. H. Ng and D. B. Spalding, Predictions of two-dimensional boundary layers on smooth walls with a two-equation model of turbulence, Imperial College, London, Mech. Eng. Dept., Rep. BL/TN/A2 (1970).
11. D. B. Spalding, The prediction of two-dimensional, steady turbulent flows, Imperial College, London, Mech. Eng. Dept. Rep. EF/TN/A-16 (1969).
12. W. P. Jones and B. E. Launder, The prediction of laminarisation with a two-equation model of turbulence, *Int. J. Heat Mass Transfer* **15**, 301–314 (1972).
13. J. Rotta, Statistische Theorie nichthomogener Turbulenz, *Z. Physik* **129**, 547–572; **131**, 51–77 (1951).
14. S. V. Patanker and D. B. Spalding, *Heat and Mass Transfer in Boundary Layers*. Morgan Grampian, London (1967).
15. B. E. Launder and D. B. Spalding, Turbulence models and their application to the prediction of internal flows, *Heat and Fluid Flow* 2.
16. E. Baker, Influence of mass transfer on surface friction at a porous surface, Ph.D. Thesis, University of London (1967).

CALCUL NUMERIQUE DES JETS PARIETAUX

Résumé—Les jets pariétaux turbulents sur des surfaces coniques représentent une situation pratique et un test important pour les méthodes théoriques de prédiction de convection turbulente. Des données expérimentales sur les champs de vitesse et sur la concentration maximale d'un gaz traceur ont été obtenues pour des surfaces coniques avec des angles variés. On montre que la prévision correcte des résultats par une hypothèse de longueur de mélange demande que la constante de longeur de mélange soit changée pour chaque angle du cone. On utilise par suite un système de modèles à deux équations qui résout deux équations différentielles additionnelles pour les propriétés locales de la turbulence. Ces modéles représentent correctement tous les résultats expérimentaux sans nécessiter l'ajustement des constantes.

NUMERISCHE BERECHNUNG VON WANDSTRAHLSTRÖMUNGEN

Zusammenfassung—Turbulente Wandstrahlströmungen an konischen Oberflächen stellen einen praktisch bedeutenden Zustand und einen wichtigen Test für theoretische Methoden dar, die zur Berechnung von turbulentem Transport benutzt werden. Experimentelle Daten der Geschwindigkeitsfelder und der maximalen Konzentration eines Indikatorgases wurden für turbulente Wandstrahlen an konischen Oberflächen verschiedener Winkel gewonnen. Es wird gezeigt, daß eine genaue Berechnung dieser Werte durch eine Mischungsweg-Hypothese eine Mischungsweg-Konstante erfordert, die für jeden Konuswinkel geändert werden muß. Daher wurde ein Satz von Zwei-Gleichungs-Modellen der Turbulenz, bei denen zwei zusätzliche Differentialgleichungen für die lokalen Turbulenzeigenschaften gelöst werden, verwendet. Diese Modelle geben die experimentellen Daten genau wieder, ohne daß Konstanten angepaßt werden müßten.

ЧИСЛЕННЫЕ РАСЧЕТЫ ПРИСТЕННЫХ СТРУЙ

Аннотация—Турбулентные пристенные струи на конических поверхностях представляют не только самостоятельный практический интерес, но используются также для проверки теоретических методов расчета турбулентного переноса. В работе получены экспериментальные данные по полям скорости и минимальной концентрации вдуваемого газа для турбулентных пристенных струй на конусах с различными углами раствора. Показано, что для правильного описания экспериментальных данных на основе гипотезы о пути смешения необходимо для каждого угла раствора конуса менять значение константы в выражении для пути смешения. В связи с этим был использован ряд моделей турбулентности, состоящих из двух дополнительных дифференциальных уравнений для локальных характеристик турбулентности. Эти модели правильно описывают экспериментальные данные и не требуют соответствующей подгонки коэффициентов.